Article

An Unexpected Role for GPR143 in Retinal Homeostasis

Dorothy Tung[1], Nicole R. Congrove[2], Anna G. Figueroa[2], Remington M Bliss[1], Tawanda Zvavamwe[1] and Brian S. McKay[1,2,*]

[1] Department of Physiology
[2] Department of Ophthalmology and Vision Science
* Correspondence: bsmckay@eyes.arizona.edu; Tel.: 1-520-5-626-1536

Abstract: Age-related macular degeneration is one of the most common causes of blindness, and the incidence exhibits profound racial bias, occurring most frequently in Caucasians. A primary cell type affected in the disease is the retinal pigment epithelium, but the etiology is unclear. The end 10% of the photoreceptor outer segments are shed each day, and the underlying retinal pigment epithelium engulfs, digests, and recycles molecules back to the sensory retina. In previous work, we showed that GPR143 signaling in response to L-DOPA may be effective in the prevention or delay of age-related macular degeneration. In this study, we explore a novel potential effector of GPR143 signaling, that of outer segment uptake and digestion. Using isolated outer segments, labelled with a pH-sensitive marker to fluoresce in lysosomes, we show that GPR143 signaling does not impact outer segment uptake, but does have a significant effect on subsequent degradation. Interestingly, GPR143 signaling did not affect the digestive capacity of the cells, marked by total proteolytic capacity and cathepsin D activity. Rather, our data suggest GPR143 improved endosomal trafficking efficiency of the phagocytosed outer segments to the lysosome. This result is similar to the effect we previously reported for GPR143 on exosome release from the endosomal compartment. Our data illustrate that GPR143 is active in endosomal traffic A single paragraph of about 200 words maximum.

Keywords: Retinal pigment epithelium of the eye; RPE; AMD (Age-related Macular Degeneration); GPR143; L-DOPA; Melanin; Ocular albinism; Exosome; Photoreceptor outer segment; Cathepsin D

1. Introduction

Age-related macular degeneration (AMD) is a leading cause of vision loss and blindness [1–3]. AMD incidence is racially biased, affecting Caucasians more frequently than all other races [1,4–6]. The reason for this bias is unknown. One of the primary cell types involved in AMD pathogenesis is the retinal pigment epithelium (RPE) [7–9]. RPE is a monolayer of cells that support the sensory retina. RPE is located between the vascular choroid and the photoreceptors, and performs a variety of functions including nutrient transport. One critical role of the RPE involves daily photoreceptor renewal by phagocytosis and digestion of spent photoreceptor outer segments (POS) [8–10]. The RPE are also heavily pigmented, suggesting they could have a role in the racial bias of AMD [11].

RPE pigmentation is critical in retinal development. Lack of pigmentation, albinism, results in a canonical retinal phenotype that includes reduced numbers of photoreceptors and ganglion cells, foveal hypoplasia, nystagmus, and loss of the uncrossed retinal projection to the brain [12–14]. Interestingly, all of these albinism related changes occur in retinal cells that never express any of the pigmentation genes. Together, these retinal changes result in low vision. One form of albinism, ocular albinism (OA), includes the complete retinal albinism phenotype described above, despite normal to near normal pigmentation in the RPE [15–20]. This creates separation between RPE pigmentation and the retinal albinism phenotype. OA is caused by a mutation in the gene encoding GPR143, a G-protein coupled receptor (GPCR) [11,21–23].

GPCRs impact and control a vast number of cellular activities and represent a large class of pharmaceutical targets. We discovered that the ligand for GPR143 is L-DOPA, a drug frequently used to treat movement disorders such as Parkinson's disease [21]. To investigate whether L-DOPA and GPR143 might affect AMD incidence, we initiated a large-scale retrospective medical record analysis to evaluate the potential association between L-DOPA prescriptions and AMD incidence [25]. Our results showed that individuals with a prescription history of L-DOPA were significantly less likely to develop AMD at any age. Further, if they did develop the disease, the initial onset of AMD was delayed by 8 years. In a small 'proof of principle' prospective study of patients undergoing treatment for neovascular AMD, L-DOPA reduced necessary anti-VEGF injections by greater than 50% [26]. L-DOPA is the only known ligand for GPR143, and GPR143 is the only known receptor for L-DOPA. Taken together, we suggest that observations of L-DOPA's effect on vision occur through GPR143 stimulation in the RPE.

GPR143 is primarily expressed in pigmented cells, such as RPE and melanocytes. The ligand for the receptor is L-DOPA, an intermediate byproduct of melanin synthesis [21,24]. Thus, cells that express GPR143, also synthesize the ligand, indicating GPR143 likely functions in an autocrine loop driven by the innate pigmentation levels of the cells expressing the receptor. In RPE, downstream effectors of GPR143 signaling include upregulation of pigment epithelial derived factor (PEDF) [26,27], and downregulation of both vascular endothelial derived factor (VEGF) [27] and exosome release [28]. Both VEGF and exosomes stimulate angiogenesis, suggesting that decreased GPR143 signaling would be detrimental and foster retinal angiogenesis. Indeed, neovascularization and retinal angiogenesis are responsible for most of vision loss in patients with AMD [29], a disease with very strong racial bias. While GPR143 is not part of the melanogenic machinery, it responds to melanogenesis, which produces L-DOPA as a biproduct, and therefore may underly the racial bias of AMD. In this study, we report an unexpected downstream activity of GPR143 signaling that occurs within the endosomal trafficking pathway, where GPR143 activity enhances POS digestion without affecting the degradative enzymes or capacity of the cells.

2. Materials and Methods

2.1. Tissue Culture

RPE were isolated as described [] and maintained in Dulbecco's modified essential medium (DMEM) supplemented with 5% fetal bovine serum (FBS). For experiments in which tyrosine concentrations were lowered, we used custom manufactured DMEM produced without tyrosine from the BIO5 media facility. Dialyzed FBS was purchased from ThermoFisher Scientific. Cells were cultured in LT media (tyrosine-free DMEM supplemented with 5 μM tyrosine, 5% dialyzed FBS, 1% antibiotic-antimycotic) for 2–4 d before experimentation.

2.2. Gel Zymography

Porcine RPE monolayers were given 20 photoreceptor outer segments (POS)/cell for 3 days in low tyrosine media (DMEM w/o tyrosine, 5% dialyzed FBS) ± 1 μM L-DOPA. Cells were rinsed with ice cold PBS and scraped in lysis buffer (25 mM Tris, 100mM NaCl, 1% NP-40, 0.1 mM Leupeptin). Protein content was determined by BCA assay (ThermoFisher Scientific, catalog # 23227). Equal amounts of protein were loaded onto a 10% SDS-polyacrylamide gels containing 0.2% gelatin. After electrophoresis, the gels were incubated in 65mM Tris (pH 7.4) with 20% glycerol for three washes of 10 minutes each. Gels were then incubated in activity buffer (0.1 M sodium phosphate buffer [pH 6.0], 1 mM EDTA, and 2 mM DTT) for 30 min at room temperature. The activity buffer was exchanged for fresh activity buffer and incubated for 48 hours at 37 °C. The gels were stained with 0.05% Coomassie Brilliant Blue and then destained with 4% methanol and 8% acetic

acid. Gels were scanned using an Epson Perfection V550 Photo scanner. Densitometry was performed using ImageJ.

2.3. Western Blot

Porcine RPE monolayers were given 20 photoreceptor outer segments (POS)/cell for 3 days in low tyrosine media (DMEM w/o tyrosine, 5% dialyzed FBS) ± 1 μM L-DOPA. Cells were rinsed with ice cold PBS and scraped in lysis buffer (50 mM Tris, 4 mM EDTA, 1% Tween 20, 1% Triton-X) and Protease Inhibitor Cocktail (Sigma–Aldrich). Protein content was determined by BCA assay (ThermoFisher Scientific, catalog # 23227). Proteins were resolved by SDS-PAGE and transferred to nitrocellulose by electric field overnight. Nitrocellulose membranes were blocked in 10% dry milk solubilized in Tris buffered saline (25 mM Tris, 150 mM NaCl, pH 7.45). The blocked membranes were incubated in primary antibody diluted in TBST containing 1% BSA for 1 hr at RT on a rocking platform. Stained membranes were rinsed four times, 5 min each, in TBST then incubated in the appropriate IRDye Secondary Antibody diluted in TBST for one hour. Immunoblots were imaged using the Licor Odyssey FC Imaging System (LI-COR Biosciences, Lincoln, Nebraska, USA).

2.4. POS Challenge

Porcine RPE were plated on a 24 well plate and grown to confluency before starting the assay. POS were counted using a hemocytometer. RPE were given 20 POS/cell in the presence or absence of 1 μM L-DOPA in LT media for three days. Old media was removed and fresh LT media ± 1 μM L-DOPA and POS Cells were added daily. Cells were incubated at 37°C.

2.5. Cathepsin Activity Fluorometric Assay

The enzymatic activity of cathepsin D in RPE cells was tested using the cathepsin D activity fluorometric assay kit (k143-100, Biovision, Milpitas, CA, USA). After a POS challenge, RPE cells were lysed cells in 50 μl of cell lysis buffer and incubated on ice for 10 min. The lysate was centrifuged at 25,000xg for 5 min and then transferred to a new tube. The cell lysate (50 μl) and Master Assay Mix (52 μl) were added to a well in a 96-well plate. The plate was incubated at 37°C for 2 hrs. The plate was read on a Flexstation 3 microplate reader with a 328-nm excitation and 460-nm emission filter. I mention that we count POS by hemocytometer in the POS challenge protocol. This is from Dorothy's thesis.

2.6. Labeling POS with pHrodo Green

To track POS degradation in the lysosome, the POS were labeled with pHrodo Green (Thermo Fisher), a pH sensitive dye that increases fluorescence intensity as pH decreases. A 0.1 M sodium bicarbonate buffer with pH 8 ± 0.05 was freshly prepared and sterile-filtered. 50 μL of DMSO was added per 100 μg of dye. The sodium bicarbonate buffer was added to the dye at 10 times the volume of the DMSO. The POS were incubated in this solution for 30 to 60 minutes in the dark. After the incubation, the solution was centrifuged at 5000xg for 10 minutes at 4°C. The supernatant was removed and the labeled POS were resuspended in sterile 5% sucrose in 5 mM HEPES.

2.7. POS Degradation Assay

Porcine RPE were plated on 8-well chambered coverglass slides and grown to confluency prior to starting the assay. Using the 40X objective, 5 phase contrast and 5 corresponding fluorescent images were taken of the wells before POS were introduced to account for cellular autofluorescence. This photography protocol was used for all experiments to maintain consistency. This represents time 0 of the degradation assay. After the POS were labeled with pHrodo Green (Thermo Fisher), they were counted using a hemocytometer and 2 POS per cell were loaded into each well along with 250 μL of LT DMEM with dFBS

and antibiotic-antimycotic. The POS were incubated with the RPE for 4 hours to permit cellular internalization. The excess POS were removed, the cells were gently rinsed, and fresh LT DMEM with dFBS was added in the presence or absence of 1 µM L-DOPA. Additional phase contrast and fluorescent images were taken at 8-hour time points up to 28 hours. The number and total area of fluorescent POS in each image were quantified using ImageJ. Over the course of this experimental series, we analyzed over 1600 images using the same settings to produce the data we present.

3. Results

3.1. Isolation of POS and RPE from Eyes.

Freshly enucleated bovine eyes were dissected to remove the anterior segment and vitreous, resulting in a retina-lined eye cup. The retina was then removed and placed in saline containing 30% sucrose. The retinas were homogenized to break off the outer segments, which were subsequently isolated by differential ultracentrifugation [30]. RPE cells were dislodged from the basement membrane by incubation with trypsin in versine.
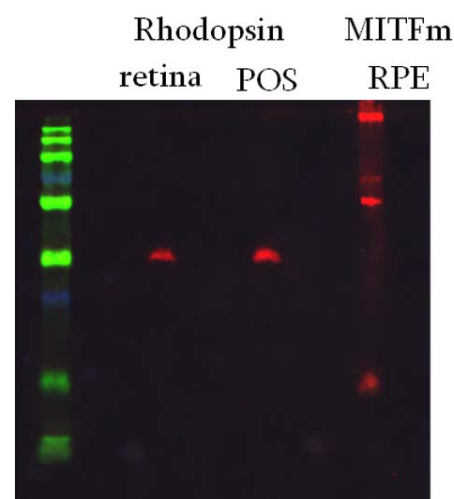

Figure 1. Purity of isolated retinal fractions. Green = Size Marker. Lanes 2 and 3 are western blots for rhodopsin in samples from total retina, or isolated POS. Lane 4 is a western blot of isolated RPE probed for MITFm.

3.2. Degradation of POS

Porcine RPE cells were incubated with fluorescently labeled POS isolated from bovine retinas, see methods for details. Figure 1 illustrates the purity of our POS and RPE preparations. Rhodopsin, a marker for photoreceptors, is present in the retinal and POS fractions, but not the RPE fraction. Similarly, MITFm, a transcription factor in the pigmentation pathway and marker for RPE, is not present in the retina or POS fractions, but is present in the RPE. This establishes the identity and purity of the isolated fractions.

We incubated 2 POS per RPE cell and allowed them to attach and undergo POS uptake and endocytosis over a 4-hour time period, at which time, excess unbound POS were removed and fresh medium was added. The number of particles in the RPE monolayer were quantified by fluorescence microscopy over time (Figure 2). The fluorescent label used was pH dependent, increasing signal as the pH decreases, so the brightness increases as the POS travel to acidic lysosomes. Therefore, the increasing brightness over time as shown, is not due to more POS in the cytoplasm, but rather movement of the POS to the acidic lysosomal compartment. As the POS are degraded in the lysosome, the brightness decreases. The peak number and brightness of fluorescent particles in lysosomes was greatest at 12 hours, then declined subsequently as POS were digested, Figures 3 and 4. L-DOPA had a significant effect on POS degradation after 12 hours, with fewer particles remaining at 20 and 28 hour time points after POS addition (figures 3 and 4). To determine

whether increased lysosomal activity was responsible for the significant increase in POS digestion, we measured mature lysosomal cathepsin D with and without GPR143 activation (Figure 5). Cathepsin D is the major RPE protease involved in POS degradation [31]. GPR143 activation by L-DOPA did not alter cathepsin D, suggesting it is unlikely that the increased POS degradation was due to increased cathepsin D activity (Figure 5).
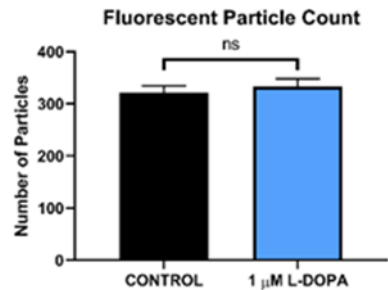

Figure 2. GPR143 does not alter POS uptake. Results illustrate total POS uptake in RPE without L-DOPA stimulation (control) or RPE stimulated with L-DOPA. The number of particles were similar in in the 2 groups. $p > 0.9$ via paired t-test analysis.
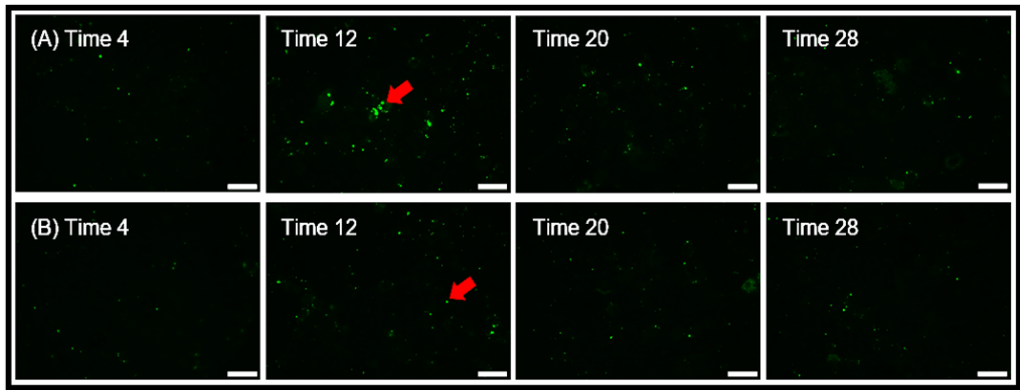

Figure 3. L-DOPA elicits an effect on POS Degradation. Series A and B are representative paired RPE monolayers, photographed at the indicated time after incubation with labelled POS. RPE were incubated with 2 POS per cell for 4 hours at which time excess POS were removed. **(A)** Control group. Images captured at 4, 12, 20, and 28 hours after POS introduction. **(B)** L-DOPA treatment group. Images captured at 4, 12, 20, and 28 hours after POS introduction. Bar = 20 μm.
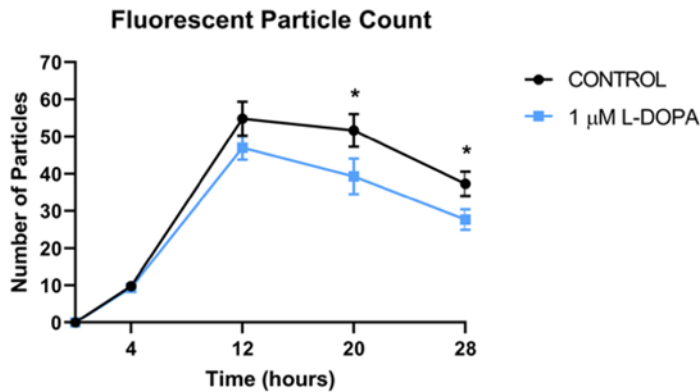

Figure 4. GPR143 Activation Enhances POS Degradation. Paired confluence monolayers of RPE were incubated with 2 POS/RPE cell. After 4 hours, excess POS were removed and numbers of cytoplasmic, fluorescent particles per field were determined. The same microscopic field was imaged over time. Data represent 4 regions per well in 4 wells of an 8-well slide. * denotes $p < 0.01$ by paired t-test analysis.
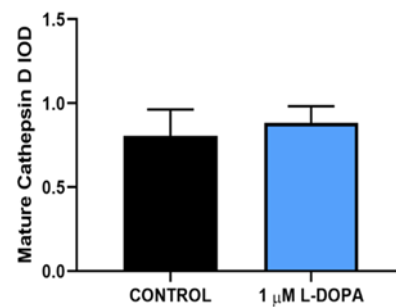
Figure 5. Active Cathepsin D Levels. Mature cathepsin D was measured in RPE lysates from paired confluent RPE by ELISA. Results shown represent mean +/- SD per mg RPE protein. The levels were not significantly different when compared using a paired T test. P>0.09.

To further understand this, we tested whether L-DOPA or POS themselves altered proteolytic activity. As shown in Figure 6, uptake of POS caused a significant increase in proteolytic activity compared to control. The combination of POS and L-DOPA together was not significantly different from the paired control cells. (Figure 6). Our results suggest that while GPR143 signaling does increase the efficiency of POS degradation, it does so without increasing the cells degrative enzymes and capacity. In previous work we demonstrated that GPR143 signaling halted exosome release in RPE [27]. Exosomes are released when the multivesicular body fuses with the plasma membrane, this is a stage of endosomal trafficking. POS are endocytosed then trafficked in the endosomal compartment to the lysosome. To test whether exosome release is an active controlled process we investigated whether time postmortem affected exosome release. Figure 8 shows results obtained using bovine eyes, and exosome collection at increasing times postmortem. All of the human eyes used in the previous work were free from ocular disease, like the young bovine eyes used here. However, they were not 'normal', they were all from enucleated eyes without a blood and oxygen supply. Figure 8 illustrates that RPE exosome release is fundamentally related to time postmortem, with increased time postmortem resulting in increasing exosome release.
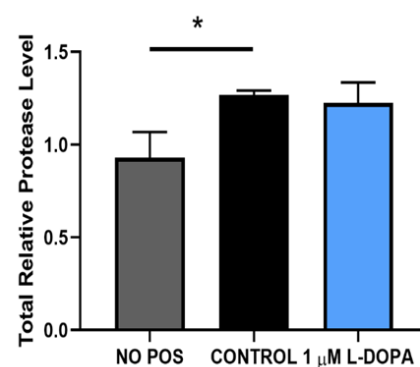

Figure 6. Comparison of RPE proteolytic capacity with POS and GPR143 activation. Control RPE (need to relabel graph) and paired cells either fed POS or POS plus L-DOPA, then lysed and total proteolytic activity was measured. Results were compared using standard paired t test. * denotes p<0.04 by paired t-test analysis.
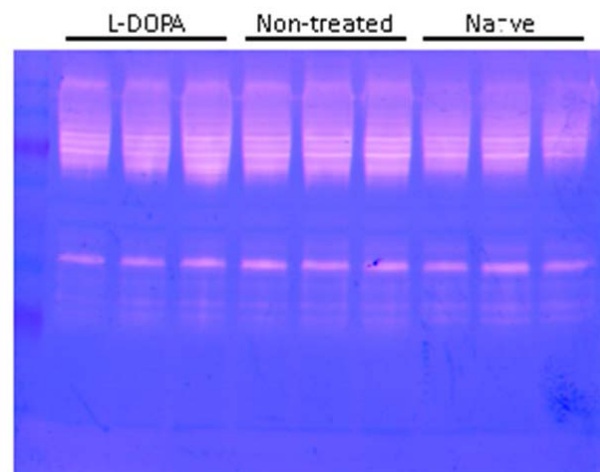
Figure 7. Unbiased Gelatin Zymography of Porcine RPE Cell Extract with Activated or Inactive GPR143. Paired monolayers were treated in triplicate with either L-DOPA +POS, POS only (untreated), or naïve, with POS not L-DOPA. Yellow arrow indicates the size of mature cathepsin D.
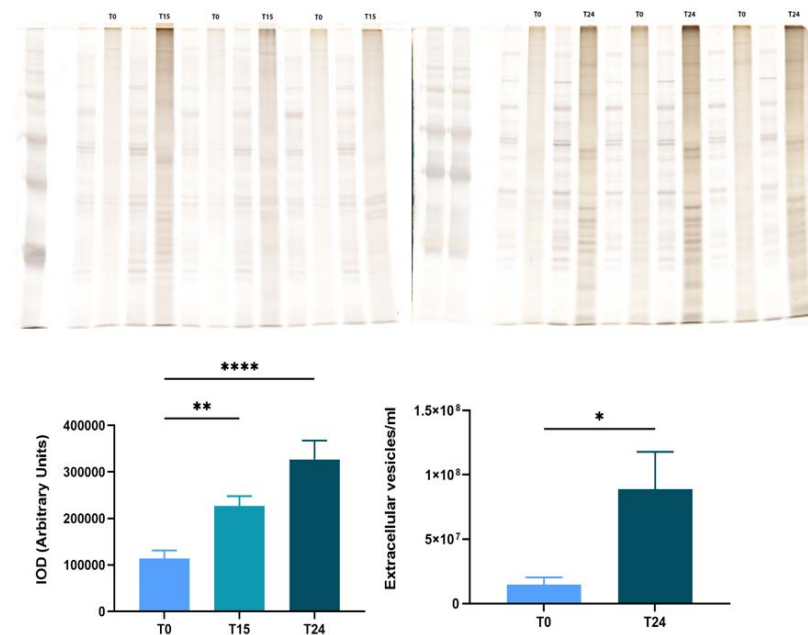

Figure 8. RPE Exosome Release is Dependent on Time Postmortem. Exosomes were isolated from pairs of bovine eyes which were dissected at different times postmortem.   Purified exosomes were quantified indirectly using unbiased total protein stain of the purified exosome sample or directly using Nanoparticle Tracking Analysis. Representative silver staining of a gel with exosome depleted conditioned medium and respective isolated exosomes at 0 and 15 hours post enucleation (A) and isolated exosomes at 0 and 24 hours post enucleation (B). Densitometry analysis of the unbiased staining of the exosome gels (C). Data analyzed by one-way ANOVA followed by Tukey's multiple comparison test; n=6-27 eyes per time point. Direct quantitation of isolated exosomes at 0 and 24 hours (D). Data analyzed by unpaired *t* test; n=12 eyes per time point.

4. Discussion

Our results illustrate an unexpected function of GPR143 signaling in POS degradation. Daily POS uptake and degradation is one of the seminal functions of RPE which supports continuous function and survival of the sensory retina [32,33]. In RPE, POS degradation has several well-defined stages: binding, which is specific through the $\alpha_v\beta_5$ integrin receptor, phagocytosis, which is POS-specific, and digestion in the lysosomal compartment [34–36]. L-DOPA treatment caused faster or more efficient POS degradation

without any measurable change in the well-studied POS degradation pathway steps; binding, uptake, or lysosomal proteolytic capacity.

We specifically measured and compared POS early phagocytosis with and without activation of GPR143 by L-DOPA. Using labelled POS that we observed, and quantified by fluorescence microscopy, there was no difference between RPE POS content with or without L-DOPA stimulation during the first 4 hours after POS addition. Results from multiple assays using different primary RPE cultures with different batches of labelled POS were consistent: GPR143 signaling does not alter the early events in POS degradation, binding and phagocytosis.

However, by 20 hours after POS introduction, the POS content of RPE was significantly reduced in RPE treated with L-DOPA compared to control. While GPR143 signaling had no effect on POS uptake, it had a significant effect on POS digestion. We hypothesized several potential mechanisms by which GPR143 signaling could increase POS degradation. The first was an increase in cathepsin D activity, the protease thought to be most active in POS degradation [31,37]. We measured active mature cathepsin D by Western Blot and found no change in the active proteases in response to GPR143 activation by L-DOPA. To determine whether increased digestion could be attributed to other proteases, we performed unbiased gelatin zymography to investigate RPE proteolytic capacity. When examining both active cathepsin D and total proteolytic activity, neither L-DOPA nor POS endocytosis affected RPE proteolytic capacity. We concluded that enhanced degradation of POS must be attributed to some other mechanism.

GPR143 may play a role in endosomal trafficking. The gene encoding GPR143 was originally identified as the cause of ocular albinism [15,16,19,20,38–40]. Loss of GPR143 signaling causes ocular albinism which is characterized by formation of 'macromelanosomes', large misshapen melanosomes which are mislocalized to the basal region of the RPE. This is likely due to a defect in endosomal trafficking caused by the loss of GPR143 signaling. Along these lines, in a previous study we showed that GPR143 signaling halted RPE exosome release using human donor eyes [28]. Exosomes are released when the multivesicular body (MVB) fuses with the plasma membrane [9,28,41,42]. The MVB is a component of the endosomal compartment, clearly impacted by GPR143 signaling [28]. Although all of the donor eyes were free from ocular disease, they were not 'normal'. They were enucleated eyes from diseased donors. To test whether exosome release is related to enucleation, we tested whether time post-enucleation of bovine eyes altered exosome release. Our results show that exosome release is directly related to time postmortem, most likely due to hypoxia, a known driver of exosome release [9,43–45]. RPE exosome release in postmortem tissue likely reflects a pathologic response to loss of blood flow and concomitant hypoxia, and should not be considered 'normal'. The effect of GPR143 activity to stop pathologic exosome release is likely beneficial.

Our previous work has suggested that activation of GPR143 signaling is beneficial in either delaying the onset of AMD, reducing the risk of developing the disease, even treating those with neovascular AMD [9,21,26]. Another way of stating reducing the probability of developing the disease, is prevention. A primary characteristic of AMD is the accumulation of drusen under the RPE [7,46–49]. In this report, we show that GPR143 signaling enhances the efficiency of the endosomal degradation pathway, this opens the possibility of activating GPR143 to reduce drusen accumulation. Future work will be to determine whether activation of GPR143 signaling reduces RPE formation of basal deposits as part of the beneficial effect on AMD.

Gabriela Figueroa, Remington M Bliss, Tawanda Zvavamwe and Brian S. McKay; Supervision, Brian S. McKay; Funding acquisition, Brian S. McKay.

References

1. Buitendijk, G.H.S.; Rochtchina, E.; Myers, C.; van Duijn, C.M.; Lee, K.E.; Klein, B.E.K.; Meuer, S.M.; de Jong, P.T.V.M.; Holliday, E.G.; Tan, A.G.; et al. Prediction of age-related macular degeneration in the general population: the Three Continent AMD Consortium. *Ophthalmology* **2013**, *120*, 2644–2655.
2. Klein, M.L.; Ferris 3rd, F.L.; Armstrong, J.; Hwang, T.S.; Chew, E.Y.; Bressler, S.B.; Chandra, S.R.; Group, A.R. Retinal precursors and the development of geographic atrophy in age-related macular degeneration. *Ophthalmology* **2008**, *115*, 1026–1031.
3. Knudtson, M.D.; Klein, R.; Klein, B.E. Physical activity and the 15-year cumulative incidence of age-related macular degeneration: the Beaver Dam Eye Study. *Br J Ophthalmol* **2006**, *90*, 1461–1463.
4. Bressler, S.B.; Munoz, B.; Solomon, S.D.; West, S.K.; Salisbury Eye Evaluation Study, T. Racial differences in the prevalence of age-related macular degeneration: the Salisbury Eye Evaluation (SEE) Project. *Arch Ophthalmol* **2008**, *126*, 241–245.
5. Wong, W.L.; Su, X.; Li, X.; Cheung, C.M.G.; Klein, R.; Cheng, C.Y.; Wong, T.Y. Global prevalence of age-related macular degeneration and disease burden projection for 2020 and 2040: A systematic review and meta-analysis. *Lancet Glob. Heal.* **2014**, *2*, e106–e116.
6. Friedman, D.S.; O'Colmain, B.J.; Muñoz, B.; Tomany, S.C.; McCarty, C.; DeJong, P.T.V.M.; Nemesure, B.; Mitchell, P.; Kempen, J.; Congdon, N.; et al. Prevalence of Age-Related Macular Degeneration in the United States. *Arch. Ophthalmol.* **2004**, *122*, 564–572.
7. Bergen, A.A.; Arya, S.; Koster, C.; Pilgrim, M.G.; Wiatrek-Moumoulidis, D.; van der Spek, P.J.; Hauck, S.M.; Boon, C.J.F.; Emri, E.; Stewart, A.J.; et al. On the origin of proteins in human drusen: The meet, greet and stick hypothesis. *Prog. Retin. Eye Res.* **2019**, *70*, 55–84.
8. Zarbin, M.A. Age-related macular degeneration: review of pathogenesis. *Eur J Ophthalmol* **1998**, *8*, 199–206.
9. Figueroa, A.G.; McKay, B.S. *A G-Protein Coupled Receptor and Macular Degeneration*; NLM (Medline), 2020; Vol. 9, pp. 1–13;.
10. Emri, E.; Kortvely, E.; Dammeier, S.; Klose, F.; Simpson, D.; Den Hollander, A.I.; Ueffing, M.; Lengyel, I.; Acar, E.; Ajana, S.; et al. A multi-omics approach identifies key regulatory pathways induced by long-term zinc supplementation in human primary retinal pigment epithelium. *Nutrients* **2020**, *12*, 1–25.
11. McKay, B.S.; Schwartz, S.G. Pigmentation and Macular Degeneration: Is There a Role for GPR143? *J. Ocul. Pharmacol. Ther.* **2016**, *32*, 3–4.
12. King, R.A.; Summers, C.G. Albinism. *Dermatol Clin* **1988**, *6*, 217–228.
13. Biswas, S.; Lloyd, I.C. Oculocutaneous albinism. *Arch Dis Child* **1999**, *80*, 565–569.
14. Oetting, W.S.; Brilliant, M.H.; King, R.A. The clinical spectrum of albinism in humans. *Mol Med Today* **1996**, *2*, 330–335.
15. Bassi, M.T.; Bergen, A.A.; Bitoun, P.; Charles, S.J.; Clementi, M.; Gosselin, R.; Hurst, J.; Lewis, R.A.; Lorenz, B.; Meitinger, T.; et al. Diverse prevalence of large deletions within the OA1 gene in ocular albinism type 1 patients from Europe and North America. *Hum Genet* **2001**, *108*, 51–54.
16. Cortese, K.; Giordano, F.; Surace, E.M.; Venturi, C.; Ballabio, A.; Tacchetti, C.; Marigo, V. The Ocular Albinism Type 1 (OA1) Gene Controls Melanosome Maturation and Size . *Invest. Ophthalmol. Vis. Sci.* **2005**, *46:*, 4358–4364.
17. Shen, B.I.N.; Samaraweera, P.; Rosenberg, B.; Orlow, S.J. Ocular albinism type 1: more than meets the eye. *Pigment Cell Res* **2001**, *14*, 243–248.
18. Lee, H.; Scott, J.; Griffiths, H.; Self, J.E.; Lotery, A. Oral levodopa rescues retinal morphology and visual function in a murine model of human albinism. *Pigment Cell Melanoma Res.* **2019**.
19. Schiaffino, M. V; Tacchetti, C. The ocular albinism type 1 (OA1) protein and the evidence for an intracellular signal transduction system involved in melanosome biogenesis. *Pigment Cell Res* **2005**, *18*, 227–233.
20. Schiaffino, M. V; D'Addio, M.; Alloni, A.; Baschirotto, C.; Valetti, C.; Cortese, K.; Puri, C.; Bassi, M.T.; Colla, C.; De Luca, M.; et al. Ocular albinism: evidence for a defect in an intracellular signal transduction system. *Nat Genet* **1999**, *23*, 108–112.
21. Lopez, V.M.; Decatur, C.L.; Stamer, W.D.; Lynch, R.M.; McKay, B.S. L-DOPA is an endogenous ligand for OA1. *PLoS Biol.* **2008**, *6*, 1861–1869.
22. McKay, B.S. Pigmentation and vision: Is GPR143 in control? *J. Neurosci. Res.* **2018**, *97*, 77–87.
23. Figueroa, A.G.; McKay, B.S. *GPR143 Signaling and Retinal Degeneration*; Springer, 2019; Vol. 1185;.
24. Goshima, Y.; Nakamura, F.; Masukawa, D.; Chen, S.; Koga, M. Cardiovascular actions of DOPA mediated by the gene product of ocular albinism 1. *J. Pharmacol. Sci.* **2014**, *126*, 14–20.
25. Brilliant, M.H.; Vaziri, K.; Connor, T.B.; Schwartz, S.G.; Carroll, J.J.; McCarty, C.A.; Schrodi, S.J.; Hebbring, S.J.; Kishor, K.S.; Flynn, H.W.; et al. Mining Retrospective Data for Virtual Prospective Drug Repurposing: L-DOPA and Age-related Macular Degeneration. *Am. J. Med.* **2016**, *129*, 292–298.

26. Figueroa, A.G.; Boyd, B.M.; Christensen, C.A.; Javid, C.G.; McKay, B.S.; Fagan, T.C.; Snyder, R.W. Levodopa Positively Affects Neovascular Age-Related Macular Degeneration. *Am. J. Med.* **2021**, *134*, 122-128.e3.

27. Falk, T.; Congrove, N.R.; Zhang, S.; McCourt, A.D.; Sherman, S.J.; McKay, B.S. PEDF and VEGF-A output from human retinal pigment epithelial cells grown on novel microcarriers. *J Biomed Biotechnol* **2012**, *2012*, 278932.

28. Locke, C.J.; Congrove, N.R.; Dismuke, W.M.; Bowen, T.J.; Stamer, W.D.; McKay, B.S. Controlled exosome release from the retinal pigment epithelium insitu. *Exp. Eye Res.* **2014**, *129*, 1–4.

29. Rein, D.B.; Wittenborn, J.S.; Burke-Conte, Z.; Gulia, R.; Robalik, T.; Ehrlich, J.R.; Lundeen, E.A.; Flaxman, A.D. Prevalence of Age-Related Macular Degeneration in the US in 2019. *JAMA Ophthalmol.* **2022**.

30. Papermaster, D.S. Preparation of retinal rod outer segments. *Methods Enzymol.* **1982**, *81*, 48–52.

31. Bosch, E.; Horwitz, J.; Bok, D. Phagocytosis of outer segments by retinal pigment epithelium: phagosome-lysosome interaction. *J Histochem Cytochem* **1993**, *41*, 253–263.

32. Sethna, S.; Chamakkala, T.; Gu, X.; Thompson, T.C.; Cao, G.; Elliott, M.H.; Finnemann, S.C. Regulation of Phagolysosomal Digestion by Caveolin-1 of the Retinal Pigment Epithelium Is Essential for Vision. *J. Biol. Chem.* **2016**, *291*, 6494–506.

33. Mao, Y.; Finnemann, S.C. Differences in Diurnal Rhythm of Rod Outer Segment Renewal between 129T2/SvEmsJ and C57BL/6J; 2016; Vol. 854;.

34. Mazzi, R.; Safa, H.; Finnemann, S.C. Understanding photoreceptor outer segment phagocytosis: Use and utility of RPE cells in culture. *Exp Eye Res* **2014**, *126*, 51–60.

35. Finnemann, S.C.; Bonilha, V.L.; Marmorstein, A.D.; Rodriguez-Boulan, E. Phagocytosis of rod outer segments by retinal pigment epithelial cells requires alpha(v)beta5 integrin for binding but not for internalization. *Proc Natl Acad Sci U S A* **1997**, *94*, 12932–12937.

36. Nandrot, E.F.; Kim, Y.; Brodie, S.E.; Huang, X.; Sheppard, D.; Finnemann, S.C. Loss of synchronized retinal phagocytosis and age-related blindness in mice lacking alphavbeta5 integrin. *J. Exp. Med.* **2004**, *200*, 1539–1545.

37. Guha, S.; Baltazar, G.C.; Tu, L.A.; Liu, J.; Lim, J.C.; Lu, W.; Argall, A.; Boesze-Battaglia, K.; Laties, A.M.; Mitchell, C.H. Stimulation of the D5 dopamine receptor acidifies the lysosomal pH of retinal pigmented epithelial cells and decreases accumulation of autofluorescent photoreceptor debris. *J. Neurochem.* **2012**, *122*, 823–833.

38. Schnur, R.E.; Gao, M.; Wick, P.A.; Keller, M.; Benke, P.J.; Edwards, M.J.; Grix, A.W.; Hockey, A.; Jung, J.H.; Kidd, K.K.; et al. OA1 mutations and deletions in X-linked ocular albinism. *Am J Hum Genet* **1998**, *62*, 800–809.

39. Schiaffino, M. V; Bassi, M.T.; Galli, L.; Renieri, A.; Bruttini, M.; De Nigris, F.; Bergen, A.A.; Charles, S.J.; Yates, J.R.; Meindl, A.; et al. Analysis of the OA1 gene reveals mutations in only one-third of patients with X-linked ocular albinism. *Hum Mol Genet* **1995**, *4*, 2319–2325.

40. Lam, B.L.; Fingert, J.H.; Shutt, B.C.; Singleton, E.M.; Merin, L.M.; Brown, H.H.; Sheffield, V.C.; Stone, E.M. Clinical and molecular characterization of a family affected with X-linked ocular albinism (OA1). *Ophthalmic Genet* **1997**, *18*, 175–184.

41. Hanson, P.I.; Cashikar, A. Multivesicular body morphogenesis. *Annu. Rev. Cell Dev. Biol.* **2012**, *28*, 337–62.

42. Eitan, E.; Suire, C.; Zhang, S.; Mattson, M.P. Impact of lysosome status on extracellular vesicle content and release. *Ageing Res. Rev.* **2016**.

43. Salomon, C.; Ryan, J.; Sobrevia, L.; Kobayashi, M.; Ashman, K.; Mitchell, M.; Rice, G.E. Exosomal Signaling during Hypoxia Mediates Microvascular Endothelial Cell Migration and Vasculogenesis. *PLoS One* **2013**.

44. Shao, C.; Yang, F.; Miao, S.; Liu, W.; Wang, C.; Shu, Y.; Shen, H. Role of hypoxia-induced exosomes in tumor biology. *Mol. Cancer* 2018.

45. Syn, N.; Wang, L.; Sethi, G.; Thiery, J.P.; Goh, B.C. Exosome-Mediated Metastasis: From Epithelial-Mesenchymal Transition to Escape from Immunosurveillance. *Trends Pharmacol. Sci.* 2016, *37*, 606–617.

46. Lengyel, I.; Tufail, A.; Hosaini, H.A.; Luthert, P.; Bird, A.C.; Jeffery, G. Association of drusen deposition with choroidal intercapillary pillars in the aging human eye. *Invest. Ophthalmol. Vis. Sci.* **2004**, *45*, 2886–2892.

47. Curcio, C.A.; Millican, C.L. Basal linear deposit and large drusen are specific for early age- related maculopathy. *Arch. Ophthalmol.* **1999**.

48. Spaide, R.F.; Ooto, S.; Curcio, C.A. Subretinal drusenoid deposits AKA pseudodrusen. *Surv. Ophthalmol.* **2018**, *63*, 782–815.

49. Curcio, C.A.; Johnson, M.; Rudolf, M.; Huang, J.D. The oil spill in ageing Bruch membrane. *Br. J. Ophthalmol.* **2011**, *95*, 1638–1645.